inorganics

MDPI

Article

Synthesis, Molecular Structure, and Computational Studies of Dinuclear d^0 Titanium(IV) Complex with P-P-Bonded Diphosphine Ligand

Tomoyuki Toda *, Yuya Toma, Miku Nishiguchi and Katsuhiko Takenaka

Department of Materials Science and Bioengineering, Nagaoka University of Technology, 1603-1 Kamitomioka, Nagaoka 940-2188, Niigata, Japan

* Correspondence: t.toda@mst.nagaokaut.ac.jp; Tel.: +81-258-47-9302; Fax: +81-258-47-9300

Abstract: Diphosphine compounds have been used as ligands for a variety of metals, and studies on their structures and reactivities are still of interest. We investigated the coordination chemistry of P–P-bonded diphosphine by conducting reactions of bis(1,1′-dibenzophospholyl) $(Db)_2P–P(Db)_2$ **1** with d^0-titanium(IV) reagents. The reaction of **1** with $TiCl_4$ afforded the dinuclear titanium complex $Cl_3Ti\{\mu\text{-}(Db)_2P–P(Db)_2\}(\mu\text{-}Cl)_2TiCl_3$ **2**. The final structure of titanium complex **2** was determined by single-crystal X-ray structural analysis. The molecular structure of the complex was found to be a dinuclear d^0-titanium complex coordinated to diphosphine on the same side, and the central titanium atoms were bridged to each other by chlorides. To further elucidate this complex, density functional theory (DFT) calculations were conducted to analyze its structure.

Keywords: diphosphine; titanium; dinuclear complex; single-crystal X-ray diffraction analysis; density functional theory

check for updates

Academic Editor: László Kótai

Received: 24 April 2025
Revised: 12 May 2025
Accepted: 13 May 2025
Published: 16 May 2025

Citation: Toda, T.; Toma, Y.; Nishiguchi, M.; Takenaka, K. Synthesis, Molecular Structure, and Computational Studies of Dinuclear d^0 Titanium(IV) Complex with P-P-Bonded Diphosphine Ligand. *Inorganics* **2025**, *13*, 169. https://doi.org/10.3390/inorganics13050169

Copyright: © 2025 by the authors. Licensee MDPI, Basel, Switzerland. This article is an open access article distributed under the terms and conditions of the Creative Commons Attribution (CC BY) license (https://creativecommons.org/licenses/by/4.0/).

1. Introduction

Phosphorus-containing compounds have been extensively studied as auxiliary ligands in transition metal complexes, making them one of the most attractive classes of compounds. These phosphorus ligands can be synthesized in various coordination geometries, including monodentate, bidentate, and polydentate forms. Many of these ligands are commercially available from chemical suppliers. Several coordination modes with metal centers are possible for bidentate phosphorus ligands. While the most well-known bidentate ligands coordinate to a single metal in a chelating fashion, they can also bridge two separate metal centers [1–5].

Diphosphine compounds, in which two phosphorus atoms are directly bonded, have a shorter interatomic distance between the two phosphorus atoms than alkyl- or aryl-bridged diphosphines, which are typically used in organometallic catalysts. Tetraphenyldiphosphine, an organo-diphosphine compound with the formula $[Ph_2P\text{-}PPh_2]$, is a centrosymmetric molecule with a P–P bond length of 2.2592 Å. The two phenyl groups on each phosphorus atom adopt a *trans* conformation to minimize the steric hindrance [6].

Several examples of early transition metal complexes, specifically Group 5 and 6 metals that are coordinated directly with P–P-bonded diphosphines, have been reported [7–23]. For instance, the diphosphine ligands form coordination complexes with Group 5 metals through the reaction of tetraphenyldiphosphine with $[Et_4N][V(CO)_6]$ or $CpM(CO)_4$ (Cp = cyclopentadienyl, M = V, Nb) [7–9]. Mizuta et al. reported the synthesis and molecular

structures of dinuclear complexes featuring 1,2-dihydro-1,2-diphenylnaphtho[1,8-cd]-1,2-diphosphole as a bridging ligand via reaction with Group 6 metal complexes [10]. The diphosphine reacts with two equivalents of $M(CO)_5(THF)$ (M = W, Mo, Cr) to afford dinuclear complexes, $(OC)_5M(\mu$-*trans*-diphosphine$)M(CO)_5$. Upon heating in a solution, these initially *trans*-coordinated complexes were partially converted to the *cis* form. The molecular structures of these complexes were determined by single-crystal X-ray crystallography. All the aforementioned Group 5 and 6 complexes were synthesized as non-d^0 metal species, suggesting that π-backbonding interactions from the metal contribute to their stability (Figure 1, top).

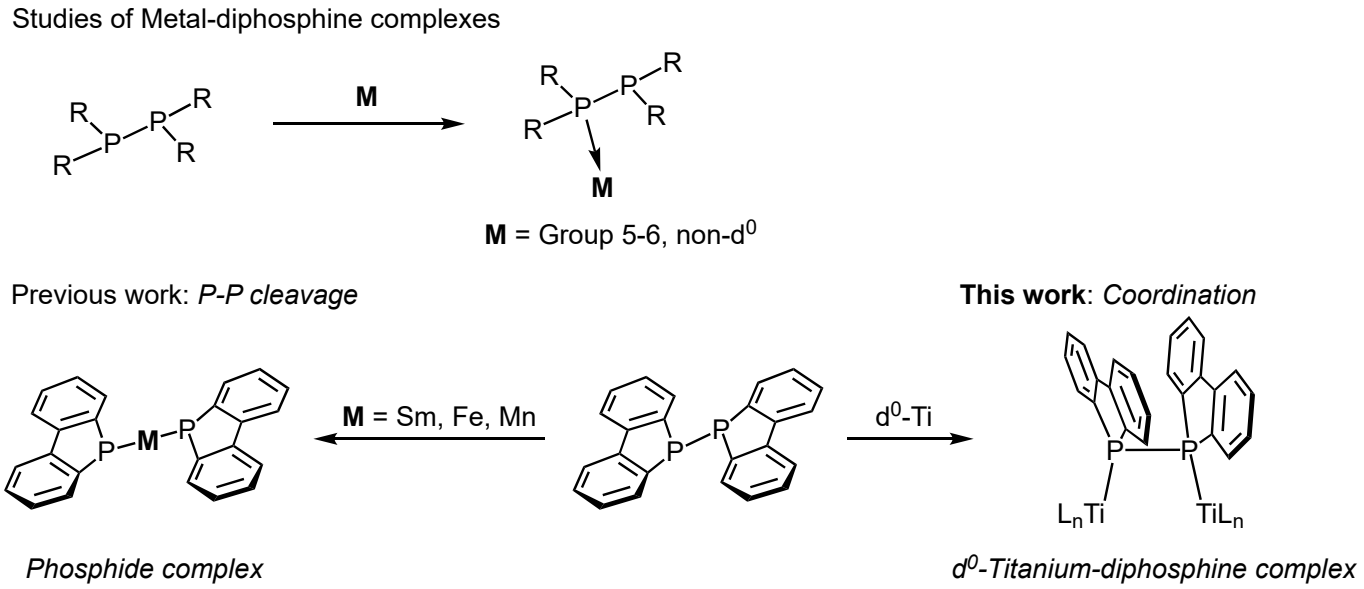


Figure 1. Studies of metal–diphosphine complexes.

As demonstrated above, the coordination mode of diphosphines is strongly influenced by the type of metal and nature of the ligands that are present on the metal center. Recently, we designed bidentate and tridentate ligands based on a dibenzophosphole backbone as a neutral phosphorus donor and synthesized Group 4 metal complexes [24–27]. Additionally, we have reported that titanium and zirconium complexes that are activated with dried modified methylaluminoxane exhibit catalytic activity for the polymerization of ethylene and 1-octene. The dibenzophosphole backbone of these ligands features a fused-ring structure with phenyl substituents on the phosphorus atoms. This structural motif reduces steric hindrance compared to the non-fused diphenylphosphine units, thereby facilitating coordination to the metal centers. In particular, for the d^0 metals that are discussed in this study, where π-backbonding interactions are not possible, minimizing the steric bulk around the phosphorus atoms is crucial for inhibiting ligand dissociation and stabilizing the complexes.

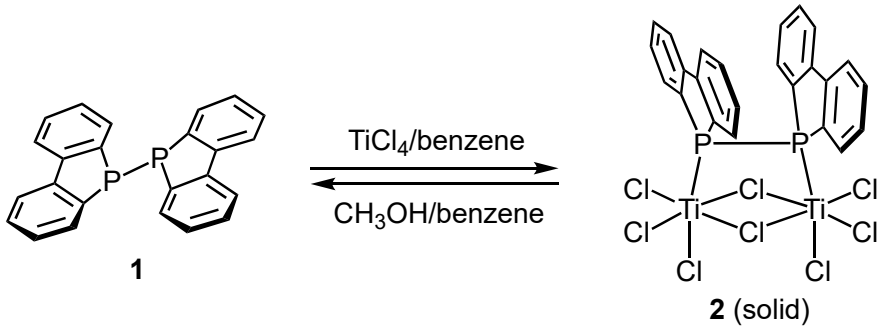
In this work, we report the synthesis and structural characterization of a dinuclear titanium complex (**2**), in which a P–P-bonded diphosphine (**1**; $(Db)_2P$-$P(Db)_2$, bis(1,1′-dibenzophospholyl)) features a dibenzophosphole unit that is coordinated to titanium centers (Figure 1, bottom right). The molecular structure of complex **2** was determined using single-crystal X-ray diffraction analysis. To the best of our knowledge, this is the first example of a direct P–P-bonded diphosphine complex with d^0 metal. The diphosphine compound **1** used in this study was previously employed in reactions with samarium(0) [28], iron(I) [29], and manganese(0) [30] species. In these cases, the P–P bond is reductively cleaved by metal electrons, leading to the coordination of phosphido anions (R_2P^-) to

the metal centers (Figure 1, bottom left). In contrast, our titanium complex retained an intact P–P bond. Additionally, computational studies were conducted to elucidate the formation mechanism, molecular structure, and electronic properties of the newly synthesized diphosphine–titanium complex in greater detail.

2. Results and Discussion

2.1. Synthesis and Structure of Dinuclear Titanium Complex **2***: Reaction of Diphosphine* **1** *with Titanium Tetrachloride*

We first investigated the reaction of P–P-bonded diphosphine compound **1** with neat titanium tetrachloride ($TiCl_4$) (Scheme 1). When diphosphine compound **1** was dissolved in benzene and treated with two equivalents of titanium tetrachloride, a black solid precipitated from the reaction mixture.



Scheme 1. Synthesis of dinuclear titanium complex **2** and reaction of **2** with methanol.

The resulting black solid was completely insoluble in conventional non-coordinating solvents, such as chloroform, dichloromethane, and toluene, rendering NMR analysis infeasible. However, a suitable single crystal for X-ray diffraction (scXRD) analysis was successfully obtained from this reaction. The molecular structure is shown at the top of Figure 2.

Figure 2 (top) reveals that the reaction yielded the dinuclear titanium complex **2** (Cl_3Ti-{μ-$(Db)_2$P-P$(Db)_2$}(μ-$Cl)_2$-$TiCl_3$). Each titanium center is coordinated by a diphosphine ligand, three terminal chloride ions, and two bridging chloride ions, adopting a distorted octahedral geometry. Structures in which a Lindner ligand coordinates to a single titanium atom in titanium chloride without forming a chelate, such as $Ph_2P(CH_2)_nPPh_2$, are extremely rare. Except for our present example, only titanate structures, such as [R_3P-Ti(μ-$Cl)_3$Ti-PR_3^-][PPh_4^+] (Ti(III), PR_3 = PEt_3 or Me_2Ph) [31] and Cl_5TiPPh_2-CH_2PHPh_2 [32], have been reported. To investigate the structure of complex **2**, we performed computational chemistry calculations using Gaussian calculations at the B3LYP/6-31G(d)/LANL2DZ level to optimize the obtained structure. The initial structure was obtained from the coordinates determined by single-crystal X-ray diffraction analysis. The results of the calculation are shown at the bottom of Figure 2. The structure adopts a C_2-symmetric conformation.

In this scXRD structure, the diphosphine ligand coordinates to the titanium center through its two phosphorus atoms with a Ti–P bond length of 2.6334(9) Å. These bond lengths are comparable to those previously reported for (*ortho*-$C_6H_4(PMe_2)_2)_nTiCl_4$ (n = 1, 2) and $[Ph_2P(CH_2)_nPPh_2]TiCl_4$ (n = 1–3) (Ti–P bond lengths: 2.5600–2.6888 Å) [32,33]. On the other hand, in the optimized structure obtained from the calculations, the Ti–P bond length was 2.794 Å, which was approximately 6% longer than that of the crystal structure. The Ti1–P1–P1#–Ti1# and C1–P1–P1#–C7 dihedral angles were 2.25(4)° and 2.9(1)°, respectively, indicating a notable structural feature. Upon coordination, the diphosphine moiety shifted from the *trans* conformation observed in free ligand **1** [30] to an eclipsed conformation in complex **2**. The P1–P1# bond length increased by 0.0216 Å upon complex formation,

corresponding to an increase of approximately 0.96% (**2**:2.2717(9) Å; **1**:2.2501(6) Å [30]). Such elongation of the P–P bond length upon complexation has also been observed in tungsten complexes with 1,2-dihydro-1,2-diphenyl-naphtho[1,8-cd]-1,2-diphosphole [10]. In this optimized structure, it was revealed that the diphosphine ligand was distorted compared to the results obtained from the scXRD analysis. The Ti1–P1–P1#–Ti1# and C1–P1–P1#–C7 dihedral angles in this optimized structure were 17.210° and 26.083°, respectively. To further investigate these distortions, we performed optimization calculations on free ligand **1**. Two optimized structures were obtained: a *gauche* conformation with a C1–P1–P1#–C7 dihedral angle of 70.531° and a *trans* conformation with an angle of 180°, as shown in Figure 3. Neither structure exhibited imaginary frequencies in the vibrational calculations, indicating that they corresponded to local minima. The P–P bond lengths were 2.274 Å in the *gauche* conformation and 2.302 Å in the *trans* conformation, suggesting free rotation within this range. Given that the P–P bond length in the optimized complex **2** was 2.290 Å, this deviation is considered to be within the margin of error rather than a significant elongation due to the decreased electron density on phosphorus upon complexation. The dibenzophosphole framework adopted a fused planar structure, and the biphenyl moiety that was attached to the P–P axis was highly rotatable. This flexibility likely enabled the coordination of Ti in the present complex.

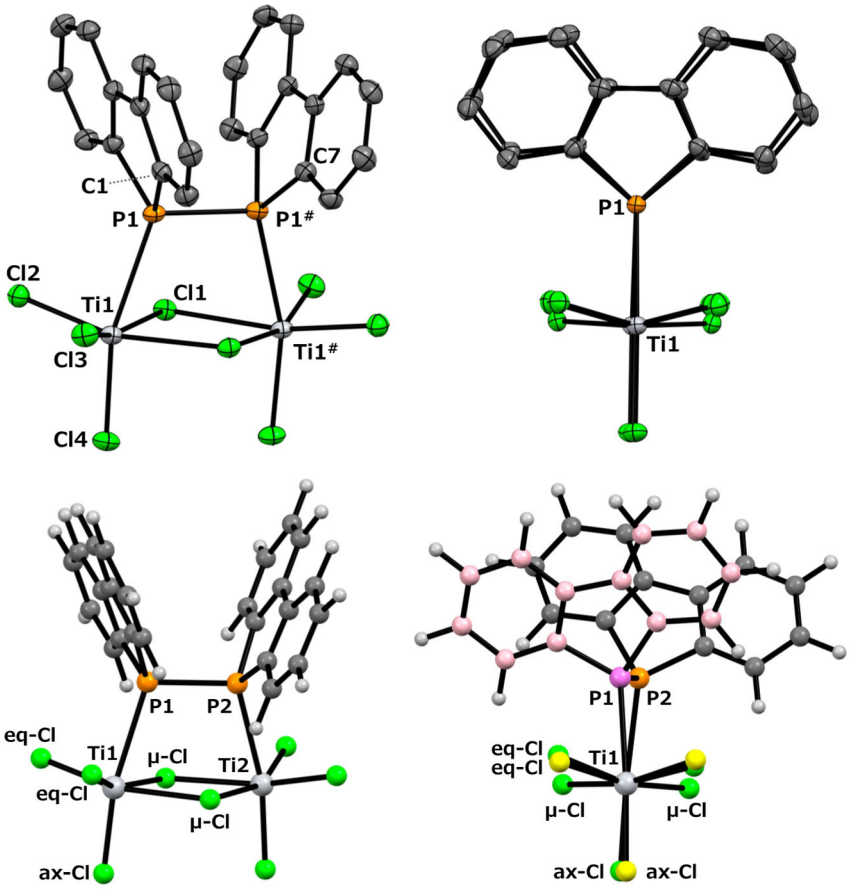


Figure 2. The molecular structure and optimized structure of dinuclear titanium complex **2**: side view (**top left**) and front view (**top right**). Thermal ellipsoids are shown at a 50% probability level. All the hydrogen atoms and crystal solvents were omitted for clarity. Side view (**bottom left**) and front view (**bottom right**), calculated using the B3LYP/6-31G(d) level of theory, employing the LANL2DZ effective core potential for titanium and chlorine atoms. For clarity, carbon (pink), phosphorus (purple), and chlorine (yellow) atoms were bonded to the front titanium (Ti1) atom.

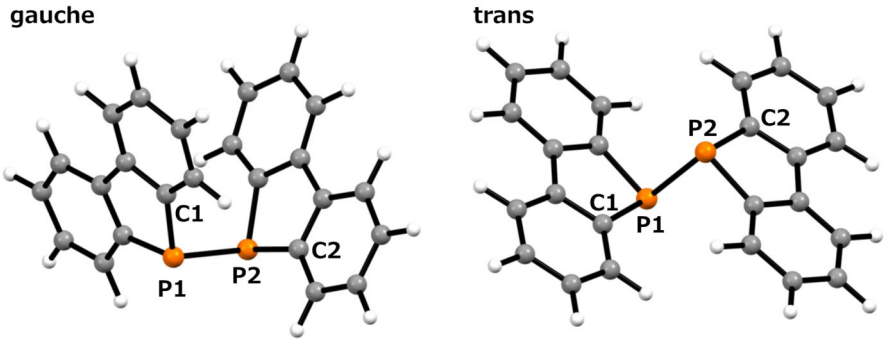


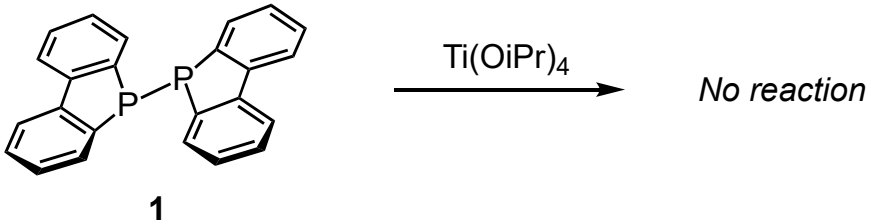
Figure 3. Optimized structure of diphosphine **1**: *Gauche* (**left**), *trans* (**right**) conformation; calculated using the B3LYP/6-31G(d) level of theory.

Focusing on the dibenzophosphole rings in scXRD, it was observed that they adopted a face-to-face orientation. The C1–C7 distance between the ipso carbons of the opposing phosphorus atoms within these rings was 3.159(4) Å. The distance between the centroids created by the aryl ring was 3.797 Å. Although these values fall within the range associated with π–π interactions, the dibenzophosphole rings are neither perfectly parallel nor in an ideal face-to-face orientation. Thus, while a weak π–π interaction may be suggested, its contribution is likely minimal. Furthermore, DFT-optimized structures exhibit a more twisted geometry, in which π–π stacking is further disfavored. These observations imply that the apparent stacking in the crystal structure is likely stabilized or induced by intermolecular packing forces within the solid state, rather than being an intrinsic feature of the isolated molecule.

To investigate the reactivity of dinuclear titanium complex **2**, its reaction with an excess amount of methanol was conducted. The initially insoluble black solid transformed into a colorless solution upon the addition of methanol. The ^{31}P NMR spectrum of the resulting solution showed a chemical shift that was identical to that of diphosphine **1**, indicating that methanol-induced decomposition occurred, leading to the release of diphosphine 1 without cleavage of the P-P bond [34–36]. According to the Hard and Soft Acids and Bases principle, titanium is classified as a hard Lewis acid with a strong oxophilicity. In contrast, methanol, as an oxygen donor, is a hard Lewis base, while the phosphorus ligand is categorized as a soft Lewis base. These characteristics suggest that a ligand substitution reaction took place on the titanium center, resulting in the dissociation of the diphosphine ligand.

2.2. Reaction of Diphosphine **1** *with Titanium Tetra(isopropoxide)*

Subsequently, the reaction of diphosphine **1** with another titanium reagent was examined (Scheme 2). Titanium tetra(isopropoxide) was employed as the titanium source. Although its Lewis acidity is lower than that of titanium tetrachloride, titanium tetra(isopropoxide) is frequently utilized as a Lewis acid catalyst [37–39], suggesting the potential formation of a coordination complex that is similar to that observed with titanium tetrachloride.



Scheme 2. Reaction of **1** with $Ti(OiPr)_4$.

Following the same experimental conditions, diphosphine **1** was mixed with titanium tetra(isopropoxide) in benzene, and the reaction progress was monitored using ^{31}P NMR spectroscopy. However, no chemical shift change was observed from the original diphosphine signal at −21.5 ppm. This result indicates that no coordination complex was formed between diphosphine **1** and titanium tetra(isopropoxide) due to reduced Lewis acidity of titanium tetra(isopropoxide). Complexes in which three or more isopropoxy groups and a neutral phosphine donor are coordinated to titanium have not been reported to date, although titanium diisopropoxide complexes featuring bidentate chelating ligands, such as phosphine–phenoxide, have been documented [40].

2.3. Energy Comparison Between the Product and the Precursor Systems

To investigate the formation mechanism of the d^0-titanium–diphosphine complex, Cl_3Ti-{μ-$(Db)_2P$–$P(Db)_2$}(μ-$Cl)_2$-$TiCl_3$, we examined the energy comparison between the between $TiCl_4$ with a free ligand and the titanium complex. For the precursor systems, the structures of $TiCl_4$ or Ti_2Cl_6(μ-$Cl)_2$ with diphosphine **1** were optimized using the B3LYP/6-31G(d) level of theory or the B3LYP/6-31G(d)/LANL2DZ level, and their vibrational frequencies were analyzed to confirm the nature of the optimized structures, followed by single-point energy calculations at the B3LYP/6-311+G(2d,p) or B3LYP/6-311+G(2d,p)/LANL2DZ level. For the formed titanium complex, the structures of complex **2** and a mononuclear coordination structure, $(Db)_2P$–$P(Db)_2$–$TiCl_4$, were optimized at the B3LYP/6-31G(d)/LANL2DZ level, their vibrational frequencies were analyzed to confirm the nature of the optimized structures, and their single-point energies were evaluated at the B3LYP/6-311+G(2d,p)/LANL2DZ level. The optimized structure of $(Db)_2P$–$P(Db)_2$–$TiCl_4$ is shown in Figure 4.

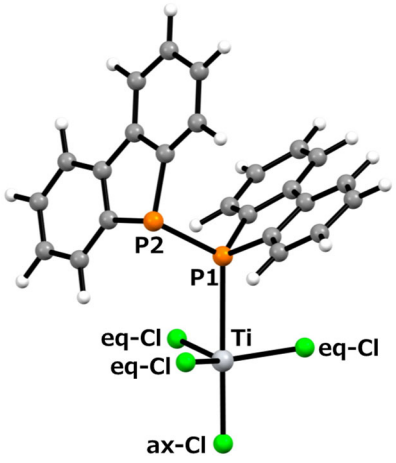


Figure 4. Optimized structure of mononuclear titanium complex $(Db)_2P$–$P(Db)_2$–$TiCl_4$, calculated using the B3LYP/6-31G(d) level of theory, employing the LANL2DZ effective core potential for titanium and chlorine atoms.

The optimization of Ti_2Cl_6(μ-$Cl)_2$ was examined using two initial structures with C_{2v} and C_{2h} symmetries, which are more closely related to the final complex structure. However, negative vibrational frequencies were observed, and the energy values of these structures were found to be higher than that of two separate $TiCl_4$ molecules. Furthermore, considering that these results do not contradict the conclusions discussed later, no further investigations were conducted.

The obtained energies are summarized in Table 1. Additionally, $\Delta E_{binding}$ and $\Delta G_{binding}$ represent the energy changes associated with the complex formation and are shown in Table 2, calculated using the equations below.

$$\Delta E_{binding} = E_{complex} - (E_{ligand} + E_{metal})$$

$$\Delta G_{binding} = G_{complex} - (G_{ligand} + G_{metal})$$

$$G_{final} = E_{6\text{-}311+G(2d,p)} + (G_{6\text{-}31G(d)} - E_{6\text{-}31G(d)})$$

Table 1. SCF energies and Gibbs energies after correction of the ligand and its metal complex, calculated at the B3LYP/6-311+G(2d,p)/LANL2DZ level. Energies are given in Hartree (Ha).

Species	$E_{6\text{-}311+G(2d,p)}$ [Ha]	G_{final} [Ha]
$TiCl_4$	−2690.66339	−2690.68944
$(Db)_2P–P(Db)_2$ **1** (*Gauche*)	−1607.24162	−1606.96617
$(Db)_2P–P(Db)_2$ **1** (*Trans*)	−1607.23930	−1606.96410
Cl_3Ti-{μ-$(Db)_2P–P(Db)_2$}(μ-$Cl)_2$-$TiCl_3$ **2**	−6988.56430	−6988.29663
$(Db)_2P–P(Db)_2–TiCl_4$	−4297.90894	−4297.64127

Table 2. Relative electronic energy ($\Delta E_{binding}$) and Gibbs free energy ($\Delta G_{binding}$) for the ligand and its metal complex. Energies are given in Ha and kcal/mol [a].

	$\Delta E_{binding}$	$\Delta G_{binding}$
Cl_3Ti-{μ-$(Db)_2P–P(Db)_2$}(μ-$Cl)_2$-$TiCl_3$ **2**	0.00411 Ha 2.6 kcal/mol	0.04843 Ha 30.4 kcal/mol
$(Db)_2P–P(Db)_2–TiCl_4$	−0.00392 Ha −2.5 kcal/mol	0.01434 Ha 9.0 kcal/mol

[a]: The energy of the free ligand was calculated using the more stable *gauche* conformation of **1**.

$E_{6\text{-}31G(d)}$: SCF energy at the 6-31G(d)/LANL2DZ level (B3LYP Energy).

$G_{6\text{-}31G(d)} - E_{6\text{-}31G(d)}$: Thermal correction term (Gibbs energy correction) at the 6-31G(d) level/LANL2DZ.

$E_{6\text{-}311+G(2d,p)}$: SCF energy at the 6-311+G(2d,p)/LANL2DZ level (B3LYP Energy).

G_{final}: Final Gibbs energy after correction.

From the obtained results, it was found that the coordination of one equivalent of titanium tetrachloride to diphosphine **1**, forming $(Db)_2P–P(Db)_2–TiCl_4$, leads to slight destabilization. Furthermore, the coordination of two equivalents of titanium tetrachloride, yielding Cl_3Ti-{μ-$(Db)_2P–P(Db)_2$}(μ-$Cl)_2$-$TiCl_3$ (**2**), results in an even greater energetic penalty, with a ΔG of +30.4 kcal/mol. This trend differs somewhat when considering the ΔE, which indicates that neither $(Db)_2P–P(Db)_2–TiCl_4$ nor Cl_3Ti-{μ-$(Db)_2P–P(Db)_2$}(μ-$Cl)_2$-$TiCl_3$ (**2**) achieves stabilization upon complex formation. Consequently, based on both ΔE and ΔG, the formation of these complexes is thermodynamically unfavorable (Figure 5).

The vibrational entropy contribution (S_vib) of 2 was calculated to be 149.3 cal/mol·K, suggesting that the complex possesses significant structural flexibility. This flexibility does not correlate with its poor solubility. Despite the positive Gibbs free energy change (+30.4 kcal/mol), complex **2** was successfully isolated as single crystals, likely due to its low solubility, which promoted precipitation from the reaction mixture. According to Le Chatelier's principle, the poor solubility may have driven crystallization, enabling the isolation of the complex despite its thermodynamic instability.

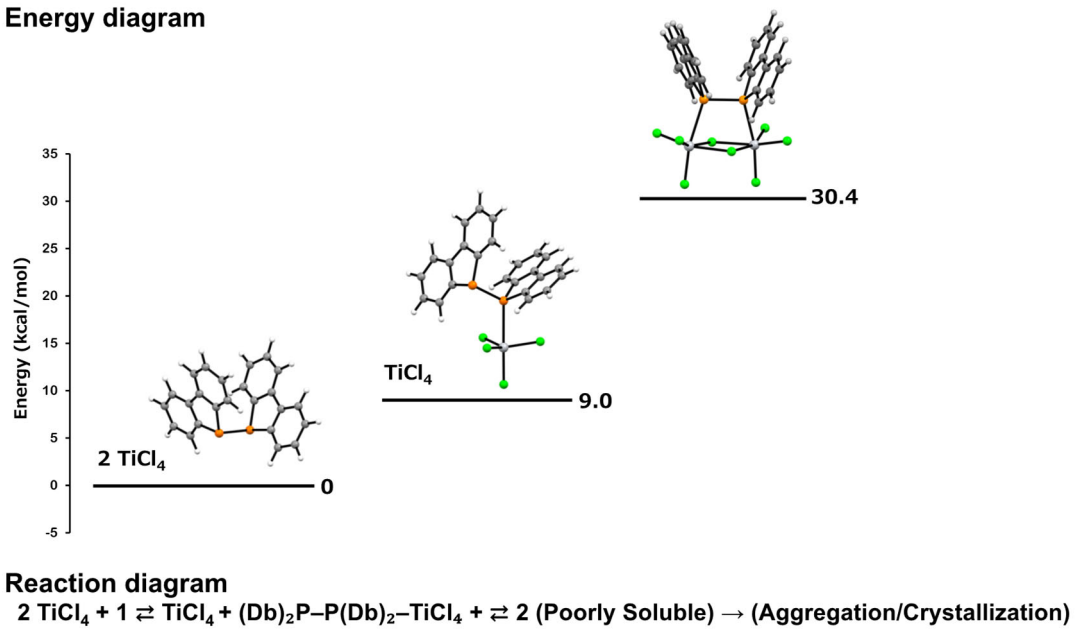


Figure 5. Energy diagrams before and after complex formation.

Next, to gain insights into why tetraisopropoxy titanium ($Ti(OiPr)_4$) did not coordinate with diphosphine **1**, we performed structure optimization on $(Db)_2P–P(Db)_2–Ti(OMe)_4$, where the four chloride ligands in $(Db)_2P–P(Db)_2–TiCl_4$ were replaced with methoxide ligands. The initial Ti–P bond length was 2.822 Å, the same as in $(Db)_2P–P(Db)_2–TiCl_4$, but during optimization, the Ti–P distance gradually increased as the energy converged, ultimately leading to a dissociated structure of diphosphine **1** and $Ti(OMe)_4$, which was found to be stable. The absence of imaginary frequencies in the vibrational analysis confirmed that this was a true minimum energy structure. This optimized structure is shown in Figure 6. From these results, we conclude that unlike $TiCl_4$, the lower Lewis acidity of $Ti(OiPr)_4$ makes it unfavorable for complex formation.

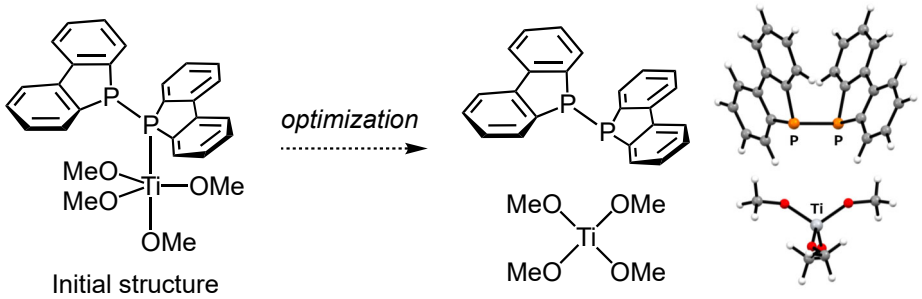


Figure 6. Optimized structure using the initial structure of $(Db)_2P–P(Db)_2–Ti(OMe)_4$, where the four chloride ligands in $(Db)_2P–P(Db)_2–TiCl_4$ were replaced with methoxide ligands, calculated using the B3LYP/6-31G(d)/LANL2DZ level of theory.

2.4. UV-Vis Spectrum of **2**

Since complex **2** was obtained as a black powder, its properties were investigated from a spectroscopic perspective. Specifically, UV-vis spectroscopy was performed, and computational studies were conducted to elucidate its electronic structure. Given that the complex was insoluble in almost all solvents except for coordinating solvents, UV-vis measurements were carried out in the solid state. The results are shown in Figure 7 (left). A weak absorption feature (Kubelka–Munk) was observed in the 500–600 nm region. To assign this absorption, the UV-vis absorption wavelengths were calculated using TD-DFT.

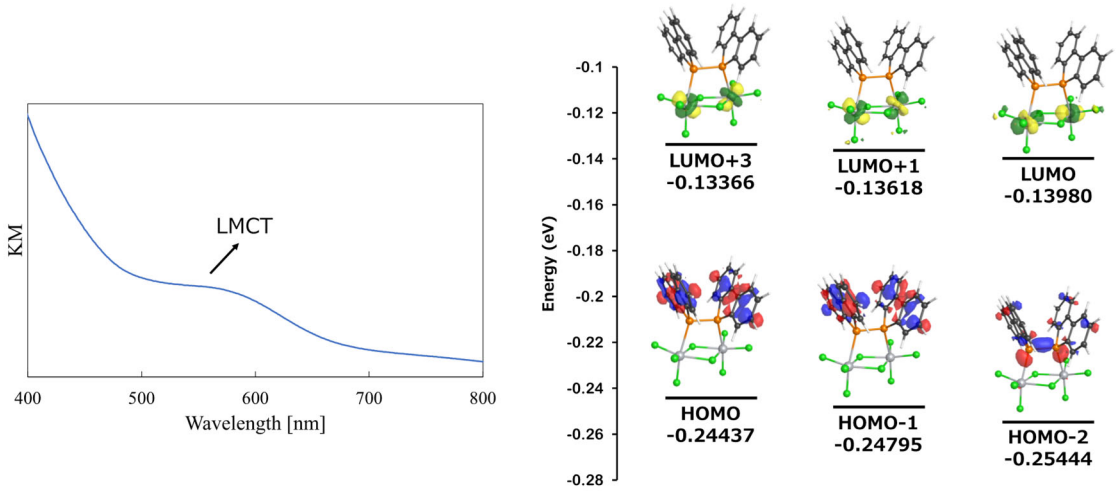


Figure 7. UV-vis spectrum of **2** in solid state (**left**) and MO diagram (**right**).

TD-DFT calculations were performed on the optimized structure of Cl_3Ti-{μ-$(Db)_2P$–$P(Db)_2$}(μ-$Cl)_2$-$TiCl_3$ (2) at the TD (NStates = 20) B3LYP/6-31G(d)/LANL2DZ level. The results predicted weak electronic transitions in the 500–600 nm region, with the most significant transitions occurring at 531.72 nm (f = 0.0018, HOMO-2 → LUMO and HOMO → LUMO transition), 516.67 nm (f = 0.0033, HOMO-2 → LUMO and HOMO → LUMO transition), and 510.09 nm (f = 0.0020, primarily HOMO → LUMO+1, with minor contributions from HOMO-2 → LUMO+1 and HOMO-1 → LUMO+3). The molecular orbitals involved in these electronic transitions are shown to the right of Figure 7. A full list of transitions is provided in the Supporting Information (Table S1).

Analysis of the molecular orbitals revealed that HOMO and HOMO-1 were delocalized over the π-system of the dibenzophosphole units, while HOMO-2 was primarily associated with the P–P bond and the lone pairs on the phosphorus atoms. In contrast, all three LUMOs contributing to the electronic transitions in the 500–600 nm region originated from the dz^2 orbital of the titanium center.

In a typical octahedral coordination environment, the six ligands induce crystal field splitting, resulting in a triply degenerate t_2g set and a doubly degenerate e_g set. Among the e_g orbitals, the dx^2-y^2 and dz^2 orbitals experience strong electrostatic repulsion from the ligands, leading to higher energy levels. The LUMO+2 (−0.13579 au) was assigned to the dx^2-y^2 orbital, supporting the interpretation that the observed transitions are ligand-to-metal charge transfer (LMCT) transitions.

To further confirm this assignment, we performed a natural transition orbital (NTO) analysis to visualize the nature of the electronic transitions. This approach allows for the visualization of the dominant electron–hole pairs in the excited state, providing a clearer understanding of the character of the transition. The results are presented in Figure 8. When comparing the molecular orbitals contributing to the TD-DFT-predicted 531.72 nm transition (HOMO-2 → LUMO and HOMO → LUMO) with the most significant NTO eigenvalue (0.97571), they were found to be in excellent agreement. Furthermore, the transition hole–particle density analysis revealed that the hole (left) is primarily localized on the ligand, while the particle (right) is distributed over the titanium center, further confirming the LMCT character of this transition. NTO analysis thus corroborated that the electronic transition at approximately 520 nm corresponds to an LMCT transition. This assignment is consistent with the weak absorption that was observed experimentally in the 500–600 nm region.

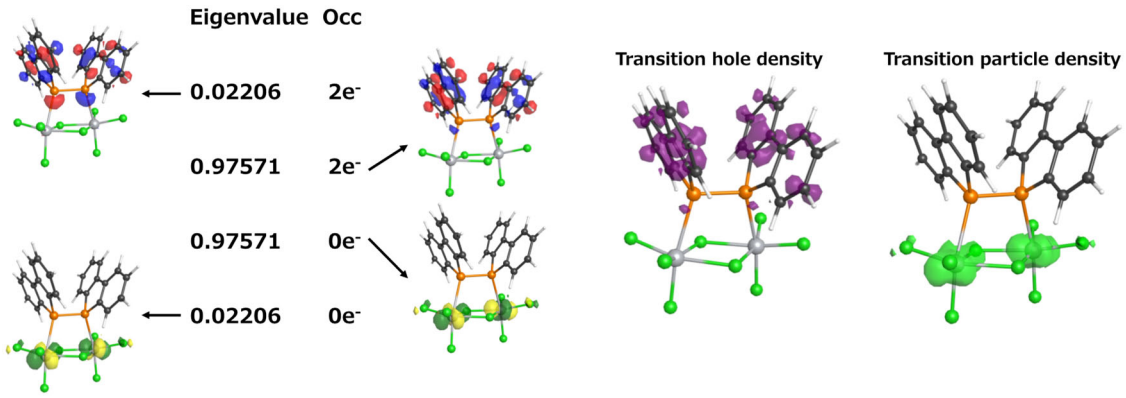


Figure 8. Natural transition orbitals (NTOs) for the electronic transition at 531.72 nm (f = 0.0018).

3. Experimental Section and Computational Details

3.1. General Procedures

All experiments were conducted either using standard Schlenk-line techniques or in a glove box under an inert atmosphere of argon. Anhydrous solvents were obtained from Fujifilm Wako Pure Chemicals and used without further purification. Nuclear magnetic resonance (NMR) measurements were recorded using JEOL ECZL-500 spectrometers (JEOL Ltd., Tokyo, Japan) in solvents such as C_6D_6, dichloromethane-d_2, or $CDCl_3$, with the solvent peak serving as the reference. Diphosphine **1** [28] was prepared in accordance with procedures described in the literature. All other chemicals and gases were used as received. The UV-vis spectrum was measured at room temperature using a Jasco V-770 spectrophotometer (JASCO Corporation, Tokyo, Japan) equipped with an integrating sphere for powdered samples. Elemental analysis was performed with a YANACO CHN Corder MT-6 (Yanaco Analytical Instruments Co., Ltd., Kyoto, Japan). The elemental analysis results of the sample showed that it exhibited very low flammability. Furthermore, the carbon (C) and hydrogen (H) contents did not match the expected values, and several possible explanations can be considered.

3.2. Reaction of Diphosphane **1** *with* **2** *Equivalent of* $TiCl_4$

To a solution of **1** (0.044 g, 0.12 mmol) in benzene (2 mL), titanium tetrachloride (0.046 g, 0.24 mmol) was added, and the mixture was stirred at room temperature. After 24 h, the disappearance of the starting material (**1**) was confirmed by ^{31}P NMR spectroscopy. The reaction mixture was concentrated to remove the solvent, washed with hexane, and dried under reduced pressure to afford dinuclear titanium complex **2** as a black solid (0.080 g, 0.096 mmol, 80%).

3.3. Reaction of Diphosphane **1** *with* $Ti(OiPr)_4$

To a solution of **1** (0.04 g, 0.11 mmol) in benzene (1 mL), titanium tetra(isopropoxide) (0.13 g, 0.46 mmol) was added, and the mixture was stirred at room temperature for 24 h. The ^{31}P NMR spectrum showed no change in the peak at −21.5 ppm, corresponding to the starting material (**1**), indicating that diphosphane **1** did not react with titanium tetra(isopropoxide).

3.4. Reaction of **2** *with Methanol*

To a solution of **1** (0.04 g, 0.11 mmol) in benzene (1 mL), titanium tetrachloride (0.10 g, 0.55 mmol) was added, and the mixture was stirred at room temperature. The reaction mixture was concentrated to remove the solvent, washed with hexane, and dried to afford complex **2** as a black solid.

Methanol (0.46 g, 13 mmol) was added to this black solid, and the mixture was stirred at room temperature. The ^{31}P NMR spectrum of the resulting solution showed only the signal corresponding to phosphine compound **1**.

3.5. X-Ray Crystallographic Studies for Dinuclear Titanium Complex **2**

A single crystal that was suitable for X-ray diffraction measurements of **2** was obtained by the reaction of **1** with $TiCl_4$ in benzene at room temperature in an argon atmosphere. X-ray diffraction data were collected at 123 K on a Rigaku XtaLAB Synergy-i diffractometer using Mo Kα radiation (λ = 0.71073 Å) (Rigaku Corporation, Tokyo, Japan). The CIF files have been deposited at the Cambridge Crystallographic Data Centre (CCDC) under the reference number CCDC 2413507, available for free via www.ccdc.cam.ac.uk/data_request/cif (or from the CCDC, 12 Union Road, Cambridge CB2 1EZ, UK; Fax: +44-1223-336033; E-mail: deposit@ccdc.cam.ac.uk).

C24 H16 Cl8 P2 Ti2, C5.369 H5.369, Cl0.42 Ti0.105, chemical_formula_weight = 835.53, crystal size 1.201 × 0.299 × 0.193 mm, monoclinic, space group I 2/a (#15), a = 13.6873(3) Å, b = 17.4631(4) Å, c = 14.8797(4) Å, β = 107.891(3)°, V = 3384.60(15) Å3, Z = 4, Dx = 1.640 g cm^{-3}. The final R(F) value was 0.0432 for reflections with I > 2σ(I), and the wR(F^2) value was 0.1304 for all data. The goodness-of-fit on F^2 was 1.063. The crystal structure was refined as a two-component twin, with scale factors of 0.6211(11) and 0.3789(11), respectively. Data collection and reduction were carried out using CrysAlisPro (Rigaku OD, Tokyo, Japan, 2022), and structure refinement was performed with SHELXL 2018/3 (Sheldrick, 2015) [41].

Twin refinement was conducted using the HKLF 5 method, allowing the two twin domains to be successfully modeled. No significant residual electron density was observed near the twin interface, with $\Delta\rho$_max = 0.714 e·Å^{-3} and $\Delta\rho$_min = −0.428 e·Å^{-3}.

All non-hydrogen atoms were refined anisotropically, while hydrogen atoms were placed geometrically and refined using a riding model.

3.6. Computational Details

All calculations were performed using the Gaussian (Revision E.01) 09 program package. Geometry optimizations were carried out at the B3LYP/6-31G(d) level of theory, employing the LANL2DZ effective core potential for titanium and chloride atoms. Frequency calculations confirmed that the optimized structures corresponded to true minima.

Electronic absorption spectra were computed using TD-DFT at the B3LYP/6-311+G(2d,p) level, employing the LANL2DZ effective core potential for titanium and chloride atoms. The lowest 20 singlet excited states were analyzed to assign the absorption bands.

The Gibbs free energy differences between the precursor and the titanium complex were evaluated at the B3LYP/6-31+G(d)/LANL2DZ level, with single-point energy corrections at the B3LYP/6-311+G(2d,p)/LANL2DZ level.

4. Conclusions

We investigated the reaction between a P–P-bonded diphosphine (**1**) and d^0-titanium compounds, elucidating the coordination behavior through NMR spectroscopy and single-crystal X-ray diffraction analysis. In the reaction of diphosphine **1** with titanium tetra(isopropoxide), no progression of the reaction was observed based on either ^1H or ^{31}P NMR spectra. In contrast, the reaction between diphosphine **1** and titanium tetrachloride proceeded, yielding black crystalline solids that were insoluble in various solvents. A single-crystal X-ray diffraction analysis revealed a dinuclear d^0-titanium complex **2** in which two phosphorus donors of the diphosphine ligand coordinated to titanium atoms, with two chloride ions bridging the titanium centers. Upon the addition of methanol to this

dinuclear complex **2**, the diphosphine ligand **1** dissociated, indicating facile substitution reactions with hard Lewis bases. These results were further analyzed using computational chemistry, revealing that while the reaction is energetically unfavorable in solution due to the lack of π-backdonation from the d^0 titanium center to the P–P-bonded diphosphine ligand, the formation of complex **2** is driven by aggregation and crystallization. Additionally, the UV-vis spectrum was identified as originating from ligand-to-metal charge transfer (LMCT). These findings underscore the complementary role of DFT in elucidating both thermodynamic and electronic aspects of the complex. Further studies on the reactivity of P–P-bonded diphosphines and related Group 4 metal complexes are currently underway.

Supplementary Materials: The following supporting information can be downloaded at: https://www.mdpi.com/article/10.3390/inorganics13050169/s1, Table S1. Molecular orbital of **2**.

Author Contributions: Conceptualization, T.T.; methodology, T.T.; validation, T.T., Y.T. and M.N.; investigation, T.T., Y.T. and M.N.; writing—original draft preparation, T.T.; writing—review and editing, K.T.; supervision, T.T. and K.T.; project administration, T.T.; funding acquisition, T.T. All authors have read and agreed to the published version of the manuscript.

Funding: This research was funded by Yoshio Nosaka Research Grant Fund for T.T.

Institutional Review Board Statement: Not applicable.

Informed Consent Statement: Not applicable.

Data Availability Statement: The original contributions presented in this study are included in the article. Further inquiries can be directed to the corresponding author.

Acknowledgments: This work was financially supported by the Yoshio Nosaka Research Grant Fund for T.T. We are grateful to H. Sato at the Rigaku Corporation for their assistance in single-crystal X-ray diffraction data collection and analysis. We would like to thank N. Kimura (Dept. of Mater. Sci. and Bioeng., Nagaoka Univ. of Tech.) for helpful discussions regarding computational chemistry. The UV-Vis measurement was performed at the Nagaoka University of Technology Analysis and Instrumentation Center, and we thank the center for the use of its facilities and equipment.

Conflicts of Interest: The authors declare no conflicts of interest.

References

1. Quin, L.D. *A Guide to Organophosphorus Chemistry*; Wiley: New York, NY, USA, 2000.
2. Kamer, P.C.J.; van Leeuwen, P.W.N.M. *Phosphorus(III) Ligands in Homogeneous Catalysis: Design and Synthesis*; Wiley: Chichester, UK, 2012. [CrossRef]
3. Chaudret, B.; Delavaux, B.; Poilblanc, R. Bisdiphenylphosphinomethane in dinuclear complexes. *Coord. Chem. Rev.* **1988**, *86*, 191–243. [CrossRef]
4. Puddephatt, R.J. Chemistry of bis(diphenylphosphino)methane. *Chem. Soc. Rev.* **1983**, *12*, 99–127. [CrossRef]
5. Balch, A.L. Binuclear, Phosphine-Bridged Complexes: Progress and Prospects. In *Homogeneous Catalysis with Metal Phosphine Complexes*; Pignolet, L.H., Ed.; Modern Inorganic Chemistry; Springer: Boston, MA, USA, 1983; pp. 167–201. [CrossRef]
6. Tam, E.C.Y.; Maynard, N.A.; Apperley, D.C.; Smith, J.D.; Coles, M.P.; Fulton, J.R. Group 14 Metal Terminal Phosphides: Correlating Structure with $|J_{MP}|$. *Inorg. Chem.* **2012**, *51*, 9403–9415. [CrossRef] [PubMed]
7. Rehder, D. Vanadaphospha-alkanes and -cycloalkanes Prepared by Photoreaction of Carbonyl-Vanadium Compounds with Tetraphenyldiphosphines. *J. Organomet. Chem.* **1977**, *137*, C25–C27. [CrossRef]
8. Bechthold, H.-C.; Rehder, D. Preparation and Ir, ^{31}P, and ^{93}Nb NMR Spectroscopic Investigation of Phosphine Derivatives of η^5-$C_5H_5Nb(CO)_4$. *J. Organomet. Chem.* **1981**, *206*, 305–315. [CrossRef]
9. Baumgarten, H.; Johannsen, H.; Rehder, D. Diphosphane, Diarsane und Distibane als Liganden in Carbonylvanadium-Komplexen. *Chem. Ber.* **1979**, *112*, 2650–2658. [CrossRef]
10. Mizuta, T.; Kunikata, S.; Miyoshi, K. Synthesis and Molecular Structures of Dinuclear Complexes with 1,2-Dihydro-1,2-diphenylnaphtho[1,8-c,d]1,2-diphosphole as a Bridging Ligand. *J. Organomet. Chem.* **2004**, *689*, 2624–2632. [CrossRef]
11. Chatt, J.; Thompson, D.T. Dinuclear Phosphorus and Arsenic Bridged Carbonyl Compounds. Part II. *J. Chem. Soc.* **1964**, 2713–2716. [CrossRef]

12. Hayter, R.G. Phosphorus- and Arsenic-Bridged Complexes of Metal Carbonyls. VI. Reactions of Tetrasubstituted Biphosphines and a Biarsine with Monomeric Metal Carbonyls. *Inorg. Chem.* **1964**, *3*, 711–717. [CrossRef]
13. Nassimbeni, L.R. The crystal structure of -tetraethyldiphosphine-bis-(pentacarbonylmolybdenum). *Inorg. Nucl. Chem. Lett.* **1971**, *7*, 187–189. [CrossRef]
14. Brockhaus, M.; Staudacher, F.; Vahrenkamp, H.; Metallorganische Lewis-Basen, X. Aufbau von Diphosphin-verbrückten, heterodinuclearen Carbonyl-Komplexen des Chroms, Mo-lybdäns und Wolframs. *Chem. Ber.* **1972**, *105*, 3716–3725. [CrossRef]
15. Staudacher, L.; Vahrenkamp, H. Metallorganische Lewis-Basen, XVII[1)] Hetero-Zweikernkomplexe des Typs $(CO)_5Cr\text{-}P(CH_3)_2\text{-}P(CH_3)_2\text{-}M$. *Chem. Ber.* **1976**, *109*, 218–228. [CrossRef]
16. Trenkle, A.; Vahrenkamp, H. Darstellung und Thermolyse P_2Me_4-verbrückter Mehrkern-Carbonylkomplexe. *Chem. Ber.* **1981**, *114*, 1366–1381. [CrossRef]
17. Trenkle, A.; Vahrenkamp, H. Metallcarbonyl-Brückenligand-Sechsringsysteme. *Chem. Ber.* **1981**, *114*, 1343–1365. [CrossRef]
18. Maigrot, N.; Charrier, C.; Richard, L.; Mathey, F. The 1,2-dihydro-1,2-diphosphete-1,4-diphosphadiene equilibrium. X-ray structures of $[\mu^2,\mu^2,\eta^1,\eta^1\text{-}(Ph)_8C_4P_4]W_2(CO)_6$ and $[\mu^1,\mu^1\text{-}(Ph)_4C_2P_2]W_2(CO)_{10}$. *Polyhedron* **1990**, *9*, 1363–1367. [CrossRef]
19. Grobe, J.; Grosspietsch, T.; Van, D.L.; Schulze, J.; Krebs, B.; Dartmann, M. Perfluormethyl-element-liganden XXXIX. Chrompentacarbonylkomplexe von Diels-Alder addukten des bis(trifluormethyl)disphosphens. *J. Organomet. Chem.* **1990**, *385*, 255–275. [CrossRef]
20. Kühl, O.; Blaurock, S.; Hey-Hawkins, E. Synthesis and molecular structure of $[Li(THF)_4][\{(CO)_4Mo\}_2(\mu\text{-}PPh_2)(\mu\text{-}PPh_2PPh_2)]$: The first compound with an 1,3-dimetalla-cyclopentaphosphane ring. *Z. Anorg. Allg. Chem.* **1999**, *625*, 1517–1521. [CrossRef]
21. Basato, M.; Brescacin, E.; Tondello, E.; Valle, G. Improved synthesis of the heteronuclear phosphido Mo–W complex $[(CO)_4Mo(\mu\text{-}PMe_2)_2W(CO)_4]$ and its use as MOCVD precursor. *Inorg. Chim. Acta* **2001**, *323*, 147–151. [CrossRef]
22. Grobe, J.; Köhne-Wächter, M.; Le Van, D. Perfluormethyl-element-liganden: XXXI. Ligandeneigenschaften von $Me_2PP(CF_3)_2$ und $Me_2AsP(CF_3)_2$. *J. Organomet. Chem.* **1985**, *280*, 331–341. [CrossRef]
23. Hinke, A.M.; Hinke, A.; Kuchen, W. Reactions of coordinated ligands II. Metal(0) carbonyl complexes with diphosphanes R(X)PP(X)R (R aryl; X Br, I, H, C_4H_9) as bridging ligands. *J. Organomet. Chem.* **1983**, *258*, 307–314. [CrossRef]
24. Toda, T.; Kasahara, Y.; Iwasaki, J.; Wakatsuki, A.; Ohta, S.; Matano, Y.; Takenaka, K. A Zirconium Complex Bearing a [NPN] Tridentate Ligand Composed of Dibenzophosphole and Pyrrolide Moieties: Synthesis, Structure, and Ethylene-Polymerization Ability. *Organometallics* **2025**, *44*, 128–136. [CrossRef]
25. Iwasaki, J.; Toda, T.; Wakatsuki, A.; Ohta, S.; Nishii, K.; Matano, Y.; Takenaka, K. Synthesis and Polymerization Activity of Phosphine-Pyrrolido [PN] Titanium and Zirconium Complexes. *Appl. Organomet. Chem.* **2025**, *39*, e7928. [CrossRef]
26. Iwasaki, J.; Kasahara, Y.; Toda, T.; Takenaka, K. 1-Octene Polymerization Catalyzed by Titanium and Zirconium Complexes Supported by [PN] or [NPN] Ligands. *Polymer J.* **2025**, *57*, 635–643. [CrossRef]
27. Iwasaki, J.; Toda, T.; Nishii, K.; Takenaka, K. Synthesis, Structure, and Polymerization Activity of $[PN]_2M(amido)_2$ (M = Ti and Zr) Complexes. *Appl. Organomet. Chem.* **2025**, *39*, e70072. [CrossRef]
28. Nief, F.; Ricard, L. Synthesis of η^1 and η^5 Complexes of Samarium(II) with Benzophospholyl Ligands. *J. Organomet. Chem.* **1994**, *464*, 149–154. [CrossRef]
29. Decken, A.; Neil, M.A.; Dyker, C.A.; Bottomley, F. Iron Complexes of the Dibenzophospholyl Ligand: A Synthetic and Crystallographic Study. *Can. J. Chem.* **2002**, *80*, 55–61. [CrossRef]
30. Decken, A.; Neil, M.A.; Bottomley, F. Synthesis and Characterization of Manganese Complexes of the Dibenzophospholyl Ligand. *Can. J. Chem.* **2001**, *79*, 1321–1329. [CrossRef]
31. Chen, L.; Cotton, F.A.; Dunbar, K.R.; Feng, X.; Heintz, R.A.; Uzelmeir, C. Preparation, Molecular and Electronic Structures, and Magnetic Properties of Face-Sharing Bioctahedral Titanium(III) Compounds: $[PPh_4][Ti_2(\mu\text{-}Cl)_3Cl_4(PR_3)_2]$. *Inorg. Chem.* **1996**, *35*, 7358–7363. [CrossRef] [PubMed]
32. Hart, R.; Levason, W.; Patel, B.; Reid, G. Synthesis, Spectroscopic and Structural Studies on Six- and Eight-Coordinate Phosphane and Arsane Complexes of Titanium(IV) Halides. *Eur. J. Inorg. Chem.* **2001**, *2001*, 2927–2933. [CrossRef]
33. Lee, K.; Wei, H.; Blake, A.V.; Donahue, C.M.; Keith, J.M.; Daly, S.R. Measurement of Diphosphine σ-Donor and π-Acceptor Properties in d^0 Titanium Complexes Using Ligand K-Edge XAS and TDDFT. *Inorg. Chem.* **2018**, *57*, 10277–10286. [CrossRef]
34. Burck, S.; Gudat, D.; Nieger, M. Diphosphanes with Polarized and Highly Reactive P−P Bonds. *Angew. Chem. Int. Ed.* **2004**, *43*, 4801–4804. [CrossRef] [PubMed]
35. Arkhypchuk, A.I.; Orthaber, A.; Ott, S. Tuning the Optical Properties of 1,1′-Biphospholes by Chemical Alterations of the P–P Bridge. *Eur. J. Inorg. Chem.* **2014**, *2014*, 1760–1766. [CrossRef]
36. Gorman, A.D.; Cross, J.A.; Doyle, R.A.; Leonard, T.R.; Pringle, P.G.; Sparkes, H.A. Phosphophosphidites Derived from BINOL. *Eur. J. Inorg. Chem.* **2019**, *2019*, 1633–1639. [CrossRef]
37. Katsuki, T.; Sharpless, K.B. The First Practical Method for Asymmetric Epoxidation. *J. Am. Chem. Soc.* **1980**, *102*, 5974–5976. [CrossRef]

38. Kumar, A.; Samuelson, A.G. Catalytic Reactions of Titanium Alkoxides with Grignard Reagents and Imines: A Mechanistic Study. *Chem. Asian J.* **2010**, *5*, 1830–1837. [CrossRef]
39. Ramachandran, P.V.; Gagare, P.D.; Sakavuyi, K.; Clark, P. Reductive Amination Using Ammonia Borane. *Tetrahedron Lett.* **2010**, *51*, 3167–3169. [CrossRef]
40. Grasset, F.; Cazaux, J.-B.; Magna, L.; Braunstein, P.; Oliver-Bourbigou, H. New Bis(aryloxy)–Ti(IV) Complexes and Their Use for the Selective Dimerization of Ethylene to 1-Butene. *Dalton Trans.* **2012**, *41*, 10396–10404. [CrossRef]
41. Sheldrick, G.M. Crystal structure refinement with SHELXL. *Acta Crystallogr. C* **2015**, *71*, 3–8. [CrossRef]

Disclaimer/Publisher's Note: The statements, opinions and data contained in all publications are solely those of the individual author(s) and contributor(s) and not of MDPI and/or the editor(s). MDPI and/or the editor(s) disclaim responsibility for any injury to people or property resulting from any ideas, methods, instructions or products referred to in the content.